



Cite this: *Chem. Commun.*, 2023, 59, 595

Received 3rd October 2022,
Accepted 13th December 2022

DOI: 10.1039/d2cc05404c

rsc.li/chemcomm

An air-stable (amino)(amido)radical was synthesized by reacting a cyclic (alkyl)(amino)carbene with carbazoyl chloride, followed by one-electron reduction. We show that an adjacent radical center weakens the amide bond. It enables the amino group to act as a strong acceptor under steric constraint, thus enhancing the stabilizing captodative effect.

Glycyl radical enzymes are important biocatalysts that enable a variety of transformations; from the reduction of nucleotides to the breakdown of inactivated hydrocarbons.¹ Their active resting state is generated by H atom abstraction at a glycine residue (Fig. 1a). The resulting C-radical **A** is highly sensitive to oxygen and the enzymatic processes work only under anaerobic conditions. Note that other reactive peptidyl radicals and related (amino)(amido) C-radicals **B** are rare in nature,^{1c,d} but are commonly involved in synthetic radical peptidic chemistry.²

The persistence of the glycyl C-radical pattern in enzymes is usually attributed to the synergic combination of an electron-donating nitrogen (blue on Fig. 1) and an electron-withdrawing carbonyl group (red), a push-pull or captodative effect.³ The protein environment also precludes the formation of C–C dimers, which are usually obtained with simpler molecular models.^{3e–i} In 2013, we took advantage of the bulky pattern of cyclic (alkyl)(amino)carbene (CAAC)^{4–6} to synthesize and isolate monomeric (amino)(carboxy) C-radical **C** under inert atmosphere.^{5a} In addition, we showed that increasing the electron-withdrawing properties of the carbonyl substituent,

such as in compound **D**, resulted in radicals with remarkable air-persistency.^{5d,7} A schematic molecular orbital analysis enables the rationalization of this effect. Indeed, the singly occupied molecular orbital (SOMO) is a bonding combination of π_{CO}^* and π_{CN}^* (Fig. 1b). An electron-withdrawing substituent on the carbonyl lowers the energy of the π_{CO}^* , thus increasing the weight of the CO fragment, which has major coefficient on oxygen. Therefore, the formal C-radical shifts to more of an O-centred radical, which is less reactive towards dioxygen.^{5d,8}

In this context, as illustrated by the high air-sensitivity of glycyl radical enzymes, amide patterns seem especially unfit for the design of bench-stable radicals; they are among both the poorest available N-donors and the weakest electron-withdrawing carbonyl groups. Herein, we challenge this paradigm and report an air-stable version of an amide-substituted

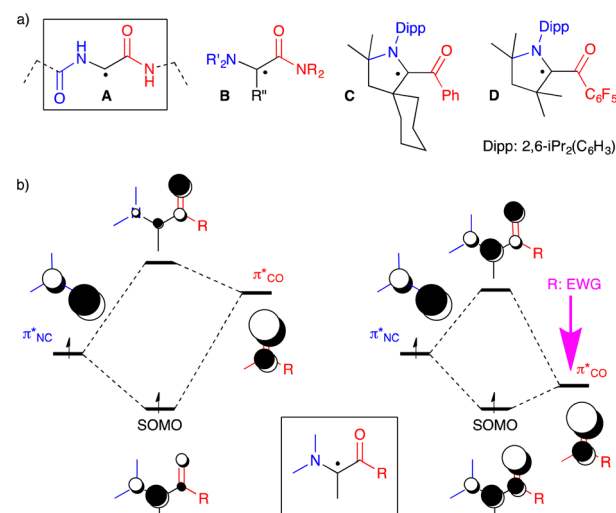


Fig. 1 (a) Glycyl radical pattern **A** in Enzymes, (amino)(amido) C-radical **B**, bottle-able push-pull C-radical **C** (air sensitive) and **D** (highly air-persistent); (b) schematic representations of SOMO of an (amino)(carbonyl) C-radical built from π_{NC}^* and π_{CO}^* , left: "classical" case, right: R is an extreme electron-withdrawing group.

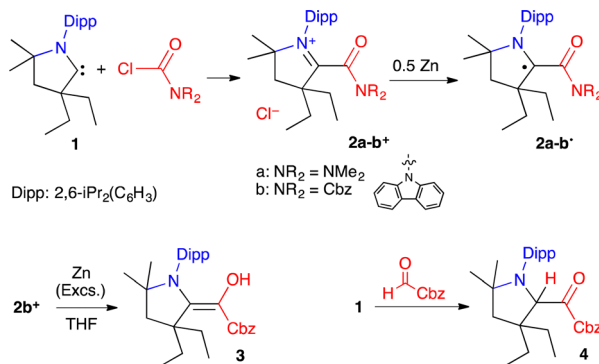
^aUCSD-CNRS Joint Research Chemistry Laboratory (IRL 3555), Department of Chemistry and Biochemistry, University of California San Diego, La Jolla, California 92093-0358, USA

^bUniversity Grenoble Alpes, CNRS, DCM, Grenoble 38000, France.
E-mail: david.martin@univ-grenoble-alpes.fr

^cUniversity Grenoble Alpes, CEA, CNRS, INAC-SyMMES, UMR 5819, Grenoble 38000, France

† Electronic supplementary information (ESI) available: Experimental procedures, analytical and computational data. CCDC 2191398 and 2191542–2191545. For ESI and crystallographic data in CIF or other electronic format see DOI: <https://doi.org/10.1039/d2cc05404c>





Scheme 1 Synthesis of radicals **2a-b[•]** and their derivatives

captodative radical. We show that the adjacent radical centre weakens the amide bond and enables the N-group to act as a strong acceptor.

We initially considered a simple *N,N'*-dimethylamido group. The chloride salt of acylium **2a**⁺ was synthesized by the addition of CAAC **1** to dimethylcarbamoyl chloride (Scheme 1). Cyclic voltammetry indicated two reversible reductions at -1.34 and -2.00 V (*versus* Fc/Fc⁺), corresponding to the formation of **2a**[•] and the enolate **2a**⁻, respectively (Fig. 2a). Radical **2a**[•] was generated *in situ* by bulk electrolysis at -1.43 V. This highly air-sensitive radical was also synthesized by chemical reduction of acylium **2a**⁺ with 0.5 equivalent of Zn(0) and isolated as a yellow solid in 88% yield. A single crystal X-ray diffraction study (Fig. 2b) revealed a dimethyl amino group with pronounced pyramidalization (sum of angles around N2: 331.6°). The lone pair of the amide nitrogen is not conjugated, but perpendicular to the carbonyl. As a result, the long C2–N2 distance (143.7 pm) is typical for a single bond and sharply contrasts with the usual bond length in planar acyclic amides (132–134 pm).⁹

Acyclic twisted amide patterns usually require the deactivation of the nitrogen with an ancillary electron-withdrawing substituent or the incorporation into an aromatic ring.^{10,11} The local environment of N2 is more reminiscent of “anti-Bredt” amides or ureas, which feature a polycyclic saturated backbone with a bridgehead nitrogen.^{12,13} These compounds are not stable when there is a significant twisting around the (OC)-N bond, as they feature both an activated electrophilic carbonyl and a nucleophilic nitrogen centre. In radical 2a•, the twist of the *N,N'*-di(methyl)amino group is maximal; however the amine acts as a strong electron-withdrawing group, which is a favourable electronic situation for a push-pull radical.⁵

We turned to a carbazole substituent to increase the electron-withdrawing capability of the carbonyl moiety. We synthesized acylium **2b**⁺ (Scheme 1). Cyclic voltammetry featured two reversible processes at -0.63 and -1.59 V, which are significantly more positive values than in the case of **2a**⁺ (Fig. 2). Radical **2b**[•] was generated *in situ* by bulk electrolysis at -0.78 V. The radical was also synthesized by chemical reduction of acylium **2b**⁺ with 0.5 equivalent of Zn(0) and isolated as a colourless solid in 84% yield. Of note, attempts to further reduce the radical with one equivalent of Zn(0) lead

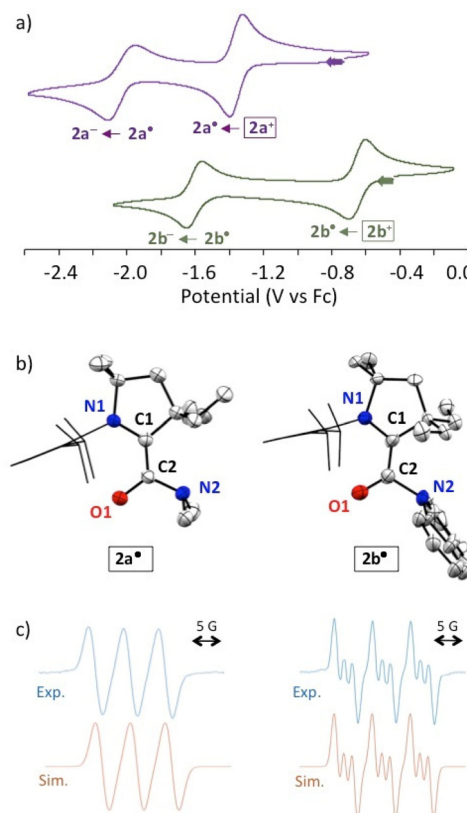


Fig. 2 (a) Cyclic voltammograms of a 1 mM solution for both the chloride salt of **2a**⁺ (top) and **2b**⁺ (below) in 0.1 M ⁷Bu₄NPF₆ acetonitrile solution at 100 mV s⁻¹ rates. (b) Solid state structures of radicals **2a**[•] and **2b**[•]. Thermal ellipsoids are set to 50% probability. Molecules of solvent, hydrogen atoms and ellipsoids on 2,6-diisopropylphenyl groups are omitted for clarity. (c) top: X-band EPR spectra of **2a**[•] (left) and **2b**[•] (right) in acetonitrile at room temperature; below: corresponding simulated spectra with the following set of parameters: **2a**[•], Lorentzian line-broadening parameter $L_w = 0.264$ and hyperfine coupling constant $a^{14}\text{N} = 15.8$ MHz (1 nucleus); **2b**[•], $L_w = 0.143$, $a^{14}\text{N} = 18.3$ MHz (1 nucleus) and 4.0 MHz (1 nucleus).

after work-up to the isolation of few crystals of the corresponding enaminol **3** (Scheme 1), which was characterized by X-ray diffraction (see ESI†). As in **2b**•, the carbazole is orthogonal to the carbonyl. This is in line with a previous study by Berkessel *et al.*, which shows that strong electron-withdrawing groups stabilize Breslow-type enols.¹⁴ Interestingly, we were also able to isolate the corresponding keto tautomer **4** from the reaction of CAAC with *N*-formyl carbazole.¹⁵

As for **2a**•, a single crystal X-ray diffraction study of **2b**• revealed a pyramidalized N2 centre (sum of angles around N2: 330.7°), a formal lone pair perpendicular to the carbonyl and a long C2–N2 distance (143.3 pm).¹⁶ Importantly, in marked contrast with sensitive radical **2a**•, **2b**• is remarkably robust towards air in the solid state and in toluene. The observation of a fast decay by EPR monitoring required heating an aerated solution in ethanol at 60 °C.

DFT¹⁷ optimized structures of **2a-b[•]** at the b3lyp/6-311g(d,p) level of theory matched the experimental solid-state geometries, as well as the EPR isotropic hyperfine coupling constants,¹⁸

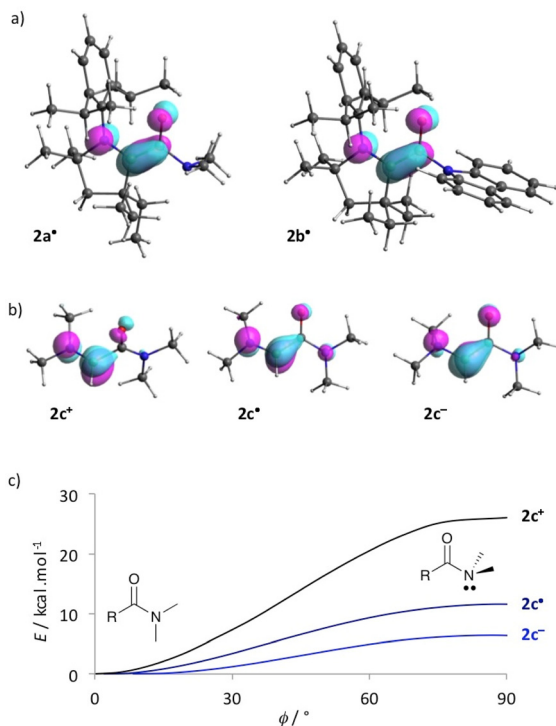


Fig. 3 (a) Optimized DFT geometry of **2a**–**b**• with representations of corresponding SOMO. (b) Optimized DFT geometry of model **2c**+, **2c**• and **2c**- with representation of corresponding LUMO, SOMO and HOMO, respectively. (c) Energy in relaxed scan optimization of **2c**+, **2c**• and **2c**- as a function of ϕ , the torsion angle between the formal N lone pair and the π_{CO} molecular orbital.

(Fig. 2c; **2a**•, computed $a(^{14}N)$: 14 MHz, experimental: 15.8 MHz; **2b**•, computed $a(^{14}N)$: 16 and 3 MHz, experimental: 18.3 and 4.0 MHz). The distribution of the Mulliken spin density (see also the representation of SOMO in Fig. 3a) is similar for both radicals (**2a**•: N1: 25%, C1: 41%, C2: 7%, O1: 26%; **2b**•: N1: 25%, C1: 37%, C2: 7%, O1: 30%). These values are reminiscent of the spin distribution of highly air persistent radical **D**, featuring a perfluorophenyl in place of the twisted amino groups. This suggests that the O-centred character of **2a**–**b**• was sufficient to disfavour triplet oxygen addition at the C1 atom.^{5d,8} Accordingly, this reaction is predicted to be endergonic for **2a**–**b**• by $\Delta G = +10.2$ and $+21.2$ kcal mol⁻¹, respectively. Thus, we considered that a single electron transfer to dioxygen was a more plausible initiation step for the pathway of decay of **2a**• in the presence of air. Indeed, radical **2a**• stands out with a very low oxidation potential (-1.34 V) when compared to previously reported CAAC-based (amino)(carboxy)radicals (from -0.2 V to -0.9 V).⁵ Note that the computed ionization potential fits well with values for parented radicals (**2a**•: 5.1, **2b**•: 5.4, C: 5.1 and **D**: 5.5 eV). However, the conformational relaxation of **2a**+, which follows the vertical ionization of **2a**•, is especially exothermic (**2a**: -28 , **2b**: -19 , C: -19 and **D**: -15 kcal mol⁻¹). Therefore, we concluded that the low oxidation potential of **2a**• was also due to the singular stability of **2a**+ compared to other acyliums of the series. Indeed, the di(methyl)amino group has a chameleonic behaviour: it is twisted and acts as a $-I$ attractor in

radical **2a**•, but it is a fully conjugated strong $+M$ donor (stronger than the aromatic carbazole of **2b**+) in acylium **2a**+

To get further insights, we considered simplified acylium, radical and enolate, **2c**+, **2c**• and **2c**- respectively, which feature a dimethylaminocarbene in place of the bulky CAAC pattern. Note that in acyliums **2a**–**c**+ the iminium moieties are perpendicular to the carbonyl, whereas the N–C–CO pattern is fully conjugated in radicals **2a**–**c**• and enolates **2a**–**c**-¹⁸. Interestingly, the small model compound **2c**• differs from CAAC-based radicals **2a**–**b**• with a fully conjugated amide moiety and only a slight pyramidalization at the nitrogen is found in **2c**-; the conformations of **2c**+, **2c**• and **2c**- with formal N2 nitrogen lone pair perpendicular to the carbonyl are transition states (Fig. 3b). However, introducing a radical or an anion in α position of the carbonyl significantly weakens the amide bond. Indeed, the formal one electron reduction to afford **2c**• (respectively **2c**-) consists in populating the LUMO of **2c**+ (SOMO of **2c**•, respectively) with anti-bonding character between C2 and N2. Accordingly, the energy barrier for full twisting dramatically decreases from **2c**+ ($\Delta G^\ddagger = +26.2$ kcal mol⁻¹) to **2c**• (+7.1 kcal mol⁻¹) and **2c**- (+6.7 kcal mol⁻¹).

Amido groups have been classified as latent rotational stereoelectronic chameleons by Alabugin *et al.*¹⁹ Misalignment of the nitrogen lone pair with the carbonyl usually requires polycyclic structures or high steric strain; however, the enhanced flexibility of an amide bond that results from an adjacent radical centre has gone unnoticed to date. Beyond implications for the design of bench-stable organic radicals, it is likely that natural evolution has already taken advantage of such redox-chameleonic behaviour.²⁰ This effect should not be overlooked in future studies on glycol enzymes or peptidyl radical chemistry.

This work was supported by the French-American cultural ex-change foundation (FACE), the NSF (CHE-1954380) and the French National Agency for Research (ANR-14-CE06-0013-01 and CBH-EUR-GS, ANR-17-EURE-0003). Thanks are due to the CECCIC and the ICMG platforms of Grenoble.

Conflicts of interest

There are no conflicts to declare.

Notes and references

- (a) J. Stubbe and W. A. van der Donk, *Chem. Rev.*, 1998, **98**, 705–762; (b) L. R. F. Backman, M. A. Funk, C. D. Dawson and C. L. Drennan, *Crit. Rev. Biochem. Mol. Biol.*, 2017, **52**, 674–695; (c) J. Hioe, G. Savasci, H. Brand and H. Zipse, *Chem. – Eur. J.*, 2011, **17**, 3781–3789; (d) J. Hioe and H. Zipse, *Faraday Discuss.*, 2010, **145**, 301–313; (e) W. Buckel and B. T. Golding, *Annu. Rev. Microbiol.*, 2006, **60**, 27–49.
- (a) C. J. Easton, *Chem. Rev.*, 1997, **97**, 53–82; (b) R. Andrukiewicz, R. Loska, V. Prisyahnyuk and K. Stalinski, *J. Org. Chem.*, 2003, **68**, 1552–1554; (c) P. Renaud and L. Giraud, *Synthesis*, 1996, 913–926; (d) C. Wyss, R. Batra, C. Lehmann, S. Sauer and B. Giese, *Angew. Chem., Int. Ed. Engl.*, 1996, **35**, 2529–2531; (e) S. Sauer, C. Staehelin, C. Wyss and B. Giese, *Chimia*, 1997, **51**, 23–24; (f) A. Schneiker, S. Góbi, P. R. Joshi, G. Bazsó, Y.-P. Lee and G. Tarczay, *J. Phys. Chem. Lett.*, 2021, **12**, 6744–6751; (g) F. J. A. Troyano, K. Merkens, K. Anwar and D. A. Gomez-Suarez, *Angew. Chem., Int. Ed.*, 2021, **60**, 1098–1115;



(h) N. Venugopal, J. Moser, M. Vojtíčková, I. Císařová, B. König and U. Jahn, *Adv. Synth. Catal.*, 2022, **364**, 405–412.

3 (a) R. W. Baldoek, P. Hudson and A. R. Katritzky, *J. Chem. Soc., Perkin Trans. 1*, 1974, 1422–1427; (b) A. T. Balaban, M. T. Caproiu, N. Negoita and R. Baican, *Tetrahedron*, 1977, **33**, 2249–2253; (c) H. G. Viehe, E. Mértnyi, L. Stella and Z. Janousek, *Angew. Chem., Int. Ed. Engl.*, 1979, **18**, 917–932; (d) H. G. Viehe, Z. Janousek, R. Mértnyi and L. Stella, *Acc. Chem. Res.*, 1985, **18**, 148–154; (e) T. H. Koch, J. A. Olesen and J. DeNiro, *J. Am. Chem. Soc.*, 1975, **97**, 7285–7288; (f) R. J. Himmelsbach, A. D. Barone, D. L. Kleyer and T. H. Koch, *J. Org. Chem.*, 1983, **48**, 2989–2994; (g) G. Gaudiano, K. Sweeney, R. C. Haltiwanger and T. H. Koch, *J. Am. Chem. Soc.*, 1984, **106**, 7628–7629; (h) O. Benson Jr., S. H. Demirdji, R. C. Haltiwanger and T. H. Koch, *J. Am. Chem. Soc.*, 1991, **113**, 8879–8886; (i) O. Benson Jr., G. Gaudiano, R. C. Haltiwanger and T. H. Koch, *J. Org. Chem.*, 1988, **53**, 3036–3045.

4 (a) V. Lavallo, Y. Canac, C. Prasang, B. Donnadieu and G. Bertrand, *Angew. Chem., Int. Ed.*, 2005, **44**, 5705–5709; (b) M. Melaimi, M. Soleilhavoup and G. Bertrand, *Angew. Chem., Int. Ed.*, 2010, **49**, 8810–8849; (c) M. Soleilhavoup and G. Bertrand, *Acc. Chem. Res.*, 2015, **48**, 256–266; (d) S. Roy, K. C. Mondal and H. W. Roesky, *Acc. Chem. Res.*, 2016, **49**, 357–369; (e) M. Melaimi, R. Jazzaar, M. Soleilhavoup and G. Bertrand, *Angew. Chem., Int. Ed.*, 2017, **56**, 10046–10068; (f) S. K. Kushvaha, A. Mishra, H. W. Roesky and K. C. Mondal, *Chem. – Asian J.*, 2022, **17**, e202101301; (g) H. Kimm and E. Lee, *Bull. Korean Chem. Soc.*, 2022, DOI: [10.1002/bkcs.12620](https://doi.org/10.1002/bkcs.12620).

5 CAAC-based organic radicals: (a) J. K. Mahoney, D. Martin, C. Moore, A. Rheingold and G. Bertrand, *J. Am. Chem. Soc.*, 2013, **135**, 18766–18769; (b) L. Jin, M. Melaimi, L. L. Liu and G. Bertrand, *Org. Chem. Front.*, 2014, **1**, 351–354; (c) Y. Li, K. C. Mondal, P. P. Samuel, H. Zhu, C. M. Orben, S. Panneerselvam, B. Dittrich, B. Schwederski, W. Kaim, T. Mondal, D. Koley and H. W. Roesky, *Angew. Chem., Int. Ed.*, 2014, **53**, 4168–4172; (d) J. K. Mahoney, D. Martin, F. Thomas, C. Moore, A. L. Rheingold and G. Bertrand, *J. Am. Chem. Soc.*, 2015, **137**, 7519–7525; (e) S. Styra, M. Melaimi, C. E. Moore, A. L. Rheingold, T. Augenstein, F. Breher and G. Bertrand, *Chem. – Eur. J.*, 2015, **21**, 8441–8446; (f) D. Munz, J. Chu, M. Melaimi and G. Bertrand, *Angew. Chem., Int. Ed.*, 2016, **55**, 12886–12890; (g) J. K. Mahoney, R. Jazzaar, G. Royal, D. Martin and G. Bertrand, *Chem. – Eur. J.*, 2017, **23**, 6206–6212; (h) M. M. Hansmann, M. Melaimi and G. Bertrand, *J. Am. Chem. Soc.*, 2017, **139**, 15620–15623; (i) M. M. Hansmann, M. Melaimi and G. Bertrand, *J. Am. Chem. Soc.*, 2018, **140**, 2206–2213; (j) P. W. Antoni and M. M. Hansmann, *J. Am. Chem. Soc.*, 2018, **140**, 14823–14835; (k) P. W. Antoni, T. Bruckhoff and M. M. Hansmann, *J. Am. Chem. Soc.*, 2019, **141**, 9701–9711; (l) V. Regnier, E. A. Romero, F. Molton, R. Jazzaar, G. Bertrand and D. Martin, *J. Am. Chem. Soc.*, 2019, **141**, 1109–1117; (m) J. Messelberger, A. Grünwald, S. J. Goodner, F. Zeilinger, P. Pinter, M. E. Miehlich, F. W. Heinemann, M. M. Hansmann and D. Munz, *Chem. Sci.*, 2020, **11**, 4138–4149.

6 For stable organic radicals based on other types of N-heterocyclic carbenes, see also: (a) J. Back, J. Park, Y. Kim, H. Kang, Y. Kim, M. J. Park, K. Kim and E. Lee, *J. Am. Chem. Soc.*, 2017, **139**, 15300–15303; (b) C. L. Deardorff, R. E. Sikma, C. P. Rhodes and T. W. Hudnall, *Chem. Commun.*, 2016, **52**, 9024–9027; (c) L. Y. M. Eymann, A. G. Tskhovrebov, A. Sienkiewicz, J. L. Bila, I. Zikhovic, H. M. Ronnow, M. D. Wodrich, L. Vannay, C. Corminboeuf, P. Pattison, E. Solari, R. Scopelliti and K. Severin, *J. Am. Chem. Soc.*, 2016, **138**, 15126–15129; (d) D. Rottshafer, B. Neumann, H.-G. Stammmer, M. van Gastel, D. M. Andrade and R. S. Ghadwal, *Angew. Chem., Int. Ed.*, 2018, **57**, 4765–4768; (e) N. M. Gallagher, H.-Z. Ye, S. Feng, J. Lopez, Y. G. Zhu, T. Van Voorhis, Y. Shao-Horn and J. A. Johnson, *Angew. Chem., Int. Ed.*, 2020, **59**, 3952–3955; (f) Y. Kim, J. E. Byeon, G. Y. Jeong, S. S. Kim, H. Song and E. Lee, *J. Am. Chem. Soc.*, 2021, **143**(23), 8527–8532; (g) J. Zhao, X. Li and Y.-F. Han, *J. Am. Chem. Soc.*, 2021, **143**, 14428–14432; (h) L. Delfau, S. Nichilo, F. Molton, J. Broggi, E. Tomás-Mendivil and D. Martin, *Angew. Chem., Int. Ed.*, 2021, **60**, 26783–26789; (i) Y. Kim and E. Lee, *Chem. – Eur. J.*, 2018, **24**, 19110–19121.

7 Stabilized oxyallyl radical cations are also parented: (a) D. Martin, C. E. Moore, A. L. Rheingold and G. Bertrand, *Angew. Chem., Int. Ed.*, 2013, **52**, 7014–7017; (b) T. Schulz, C. Farber, M. Leibold, C. Bruhn, W. Baumann, D. Selent, T. Porsch, M. C. Holthausen and U. Siemeling, *Chem. Commun.*, 2013, **49**, 6834; (c) V. Regnier and D. Martin, *Org. Chem. Front.*, 2015, **2**, 1536–1545; (d) V. Regnier, F. Molton, C. Philouze and D. Martin, *Chem. Commun.*, 2016, **52**, 11422–11425; (e) M. Devillard, V. Regnier, M. Tripathi and D. Martin, *J. Mol. Struct.*, 2018, **1172**, 3–7; (f) M. Tripathi, V. Regnier, Z. Ziani, M. Devillard, C. Philouze and D. Martin, *RSC Adv.*, 2018, **8**, 38346–38350; (g) E. Tomás-Mendivil, M. Devillard, V. Regnier, J. Pecaut and D. Martin, *Angew. Chem., Int. Ed.*, 2020, **59**, 11516–11520.

8 The low reactivity of O-centered radicals with dioxygen is usually paralleled with the extreme weakness of O–O bonds. For a discussion, see: (a) R. G. Hicks, *Org. Biomol. Chem.*, 2007, **5**, 1321–1338; (b) I. Ratera and J. Veciana, *Chem. Soc. Rev.*, 2012, **41**, 303–349.

9 F. H. Allen, O. Kennard, D. G. Watson, L. Brammer, A. G. Orpen and R. Taylor, *J. Chem. Soc., Perkin Trans. 2*, 1987, S1.

10 G. Meng, J. Zhang and M. Szostak, *Chem. Rev.*, 2021, **121**, 12746–12783.

11 For a unique case of twisted N-alkyl amide, in the solid-state structure of dimeric assemblies, see: S. E. Snyder, B.-S. Huang, Y. W. Chu, H.-S. Lin and J. R. Carey, *Chem. – Eur. J.*, 2012, **18**, 12663–12671.

12 H. K. Hall and A. El-Shekeil, *Chem. Rev.*, 1983, **83**, 549–555.

13 (a) K. Tani and B. M. Stoltz, *Nature*, 2006, **441**, 731–734; (b) J. Clayden and W. J. Moran, *Angew. Chem., Int. Ed.*, 2006, **45**, 7118–7120; (c) T. Ly, M. Krout, D. K. Pham, K. Tani, B. M. Stoltz and R. R. Julian, *J. Am. Chem. Soc.*, 2007, **129**, 1864–1865.

14 M. Paul, J.-M. Neudörfl and A. Berkessel, *Angew. Chem., Int. Ed.*, 2019, **58**, 10596–10600.

15 (a) D. Martin, V. Lavallo, Y. Canac and G. Bertrand, *J. Am. Chem. Soc.*, 2014, **136**, 5023–5030; (b) M. Paul, M. Breugst, J.-M. Neudörfl, R. B. Sunoj and A. Berkessel, *J. Am. Chem. Soc.*, 2016, **138**, 5044–5051.

16 CCDC 2191398 and 2191542–2191545 contain the supplementary crystallographic data for this paper†.

17 M. J. Frisch, G. W. Trucks, H. B. Schlegel, G. E. Scuseria, M. A. Robb, J. R. Cheeseman, et al., *Calculations were performed with the Gaussian suite of programs: Gaussian09, Revision D.01*, Gaussian, Inc., Wallingford CT, 2009. See ESI for complete citation.

18 Experimental values for isotropic hyperfine constants were extracted from EPR spectra by fitting with the EasySpin simulation package: S. Stoll and A. Schweiger, *J. Magn. Reson.*, 2006, **178**, 42–55.

19 S. Z. Vatsadze, Y. D. Loginova, G. dos Passos Gomes and I. V. Alabugin, *Chem. – Eur. J.*, 2017, **23**, 3225–3245.

20 O. A. Levitskiy, A. V. Bogdanov, I. A. Klimchuk and T. V. Magdesieva, *Chem. – Eur. J.*, 2020, **26**, 6793–6804.

